

Performance of the e2v 1.2 GPixel cryogenic camera for the J-PAS 2.5m survey telescope

M S Robbins^{*a}, M Bastable^a, A Bates^a, M Dryer^a, S Eames^a, G Fenemore-Jones^a, G Haddow^a, P R Jordan^a, B Lane^a, A Marin-Franch^b, J Mortimer^a, I Palmer^a, N Puttay^a, R Renshaw^a, M Smith^a, A Taylor^a, K Taylor^c, J Tearle^a, P Weston^a, P Wheeler^a, J Worley^a

^a e2v, Waterhouse Lane, Chelmsford, Essex, CM1 2QU, UK; ^b Centro de Estudios de Fisica del Cosmos de Aragon, Plaza San Juan 1 piso 2, 44001 Teruel, Spain; ^c Universidade de Sao Paulo, IAG, Rua do Matao, 1226, Sao Paulo, 05508-900, Brazil

ABSTRACT

The J-PAS project will perform a five-year survey of the northern sky from a new 2.5m telescope in Teruel, Spain. In this paper the build and factory testing of the commercially supplied cryogenic camera is described. The 1.2 Giga-pixel focal plane is contained within a novel liquid-nitrogen cooled vacuum cryostat, which maintains the flatness for the cooled, 0.45m diameter focal plane to better than 27 μm peak to valley. The cooling system controls the focal plane to a temperature of -100°C with a variation across the focal plane of better than 2.5°C and a stability of better than $\pm 0.5^\circ\text{C}$ over the long periods of operation required. The proximity drive electronics achieves total system level noise performance better than 5 e⁻ from the 224-channel CCD system.

Keywords: cryogenic camera, CCD, J-PAS, survey, low noise, gigapixel, mosaic, FPA.

1. INTRODUCTION

The J-PAS (Javalambre Physics of the accelerating universe Astronomical Survey) project requires a large focal plane mosaic camera as the primary instrument for the 2.5m telescope operating in Spain. e2v technologies have designed and are supplying the camera unit and cooling facility (Cryocam). Cryocam forms a part of the JPCam [1], which also includes the mechanical subsystem on the telescope, including the shutter and filter assemblies. Cryocam utilises fourteen 82 Megapixel science CCDs, together with auxiliary wavefront and autoguide devices, on a precision focal plane, and must operate with high performance and minimum maintenance for at least ten years. All design reviews have been completed for Cryocam and the assembly, integration, verification and test phase of the program is nearing completion. Factory acceptance testing will be undertaken in June 2016 with delivery planned for the end of the month. This paper describes how the challenging user requirements have been met by Cryocam, including the demanding mechanical and cooling requirements. Results from the verification testing activities are presented, including the advanced metrology performed on the focal plane, cooling trials performed to date, and performance of the electronics at a system level.

2. AN OVERVIEW OF CRYOCAM

Details of the Cryocam have been presented at previous conferences (e.g. [2]). A summary of the system architecture is presented in Figure 1 and a simplified product breakdown structure shown in Figure 2. The e2v camera consists of the following main components; sets of three CCD types in custom packages (fourteen 9kx9k e2v CCD290-99 full frame science devices, eight 2kx2k e2v CCD44-82 frame-transfer devices for wavefront sensing and four 1kx1k e2v CCD47-20 frame-transfer devices for autoguiding) mounted on a precision focal plane cold plate, a cryogenic vacuum cryostat with precision kinematic mounts for the focal plane, liquid nitrogen delivery and control system, local low-noise electronics, CCD interface electronics and data transfer electronics, all designed for this application, interfaces to the mounting system and telescope, together with system control software and an application programming interface (API) for image acquisition and camera operation.

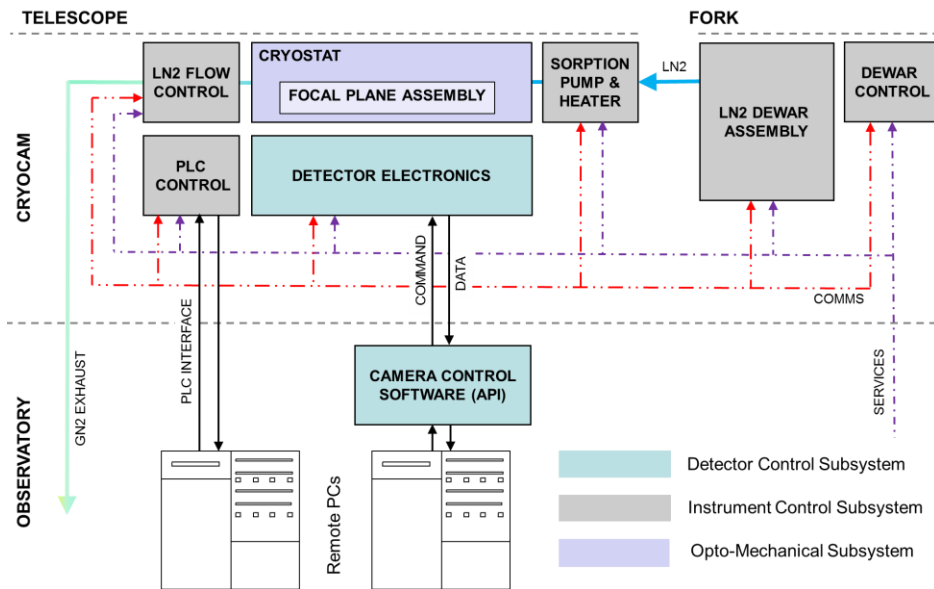


Figure 1 Cryocam systems architecture

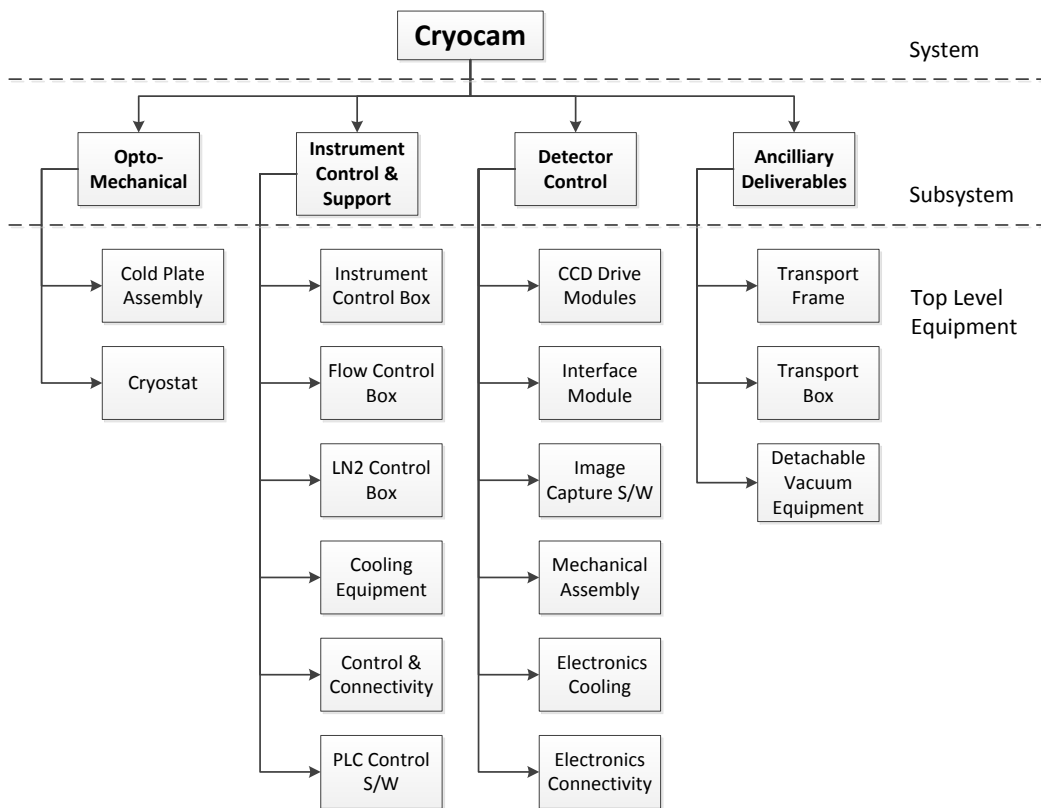


Figure 2 Simplified product breakdown structure broken down to the first level of equipment.

3. THE OPTO-MECHANICAL SUBSYSTEM

3.1 Opto-Mechanical Description

The focal plane assembly is housed within a custom vacuum cryostat. The cryostat mounted within the metrology equipment, is shown in Figure 3. Inside the cryostat is a copper ring through which mixed phase nitrogen is passed. The cold plate of the focal plane is attached to this ring by using thermal straps designed to minimise distortion of the cold plate. The chamber is initially evacuated by a local turbo pump prior to use but is not active during telescope operation. A custom sorption-pump is also fitted and maintains vacuum during normal use. A short evacuation and cooldown time and low-maintenance operation are important elements of the design. The performance of the sorption pump will be covered in Section 4.

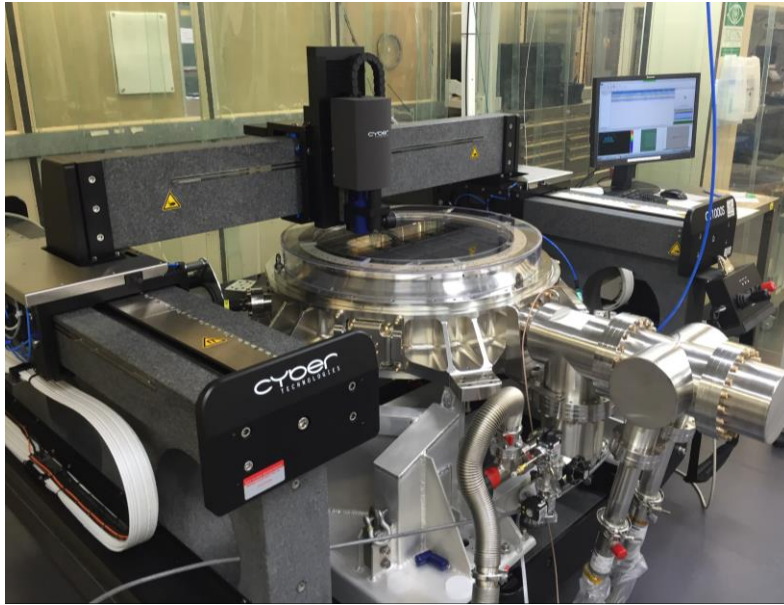


Figure 3 The deliverable cryostat on the CT1000 non-contact measuring system for geometric measurements whilst the focal plane is at -110°C .

3.2 Geometric Verification

Most of the geometric requirements have been verified using a Cyber Technologies CT1000 non-contact 3D measurement system. This uses a “chromatic white sensor”, which measures using a light point and a spectrometer. Light consisting of different wavelengths is projected on different height levels and the spectrometer analyses intensity versus wavelength. A height reading is generated when the intensity of a certain wavelength reaches a maximum in the spectrometer. The Z axis accuracy is specified to be $1.5\mu\text{m}$. The X and Y axis accuracy is specified to be under $10\mu\text{m}$. The fiducial positions were measured for the 14 science CCDs, where fiducial positions are accurate to 1 to $2\mu\text{m}$.

One of the most demanding requirements is the flatness of the focal plane itself. The focal plane plate with integrated light baffle, inside the cryostat, is shown in Figure 4. The whole assembly, including the focal plane and mounting structures have been carefully designed to minimise distortion on cooling to the operating temperature of -110°C . Measurements of the flatness of this focal plane made cold are also shown in Figure 4. The flatness achieved was $27\mu\text{m}$ peak to valley for the array of science devices, significantly better than the specifications of $40\mu\text{m}$ and the target of $30\mu\text{m}$. Including the auxiliary CCDs, the entire focal plane flatness was $58\mu\text{m}$, within the requirement of $200\mu\text{m}$. The excellent flatness of the focal plane has been achieved by careful consideration of all the interactions, including those forces exerted by the thermal straps connecting the plate to the cold ring.

Other geometric requirements have also been verified with the focal plane operating cold, including the position of the light baffle apertures and the focal plane tilt and position relative to the cryostat mounting interfaces. The distance between the centre dowel of the focal plane and the central point created by the three mounting dowels is 0.39 mm, meeting the requirement of 0.5 mm. The absolute rotation of the focal plane relative to the mounting dowels is less than 0.005 degrees which exceeds the requirement of +/-0.5 degrees.

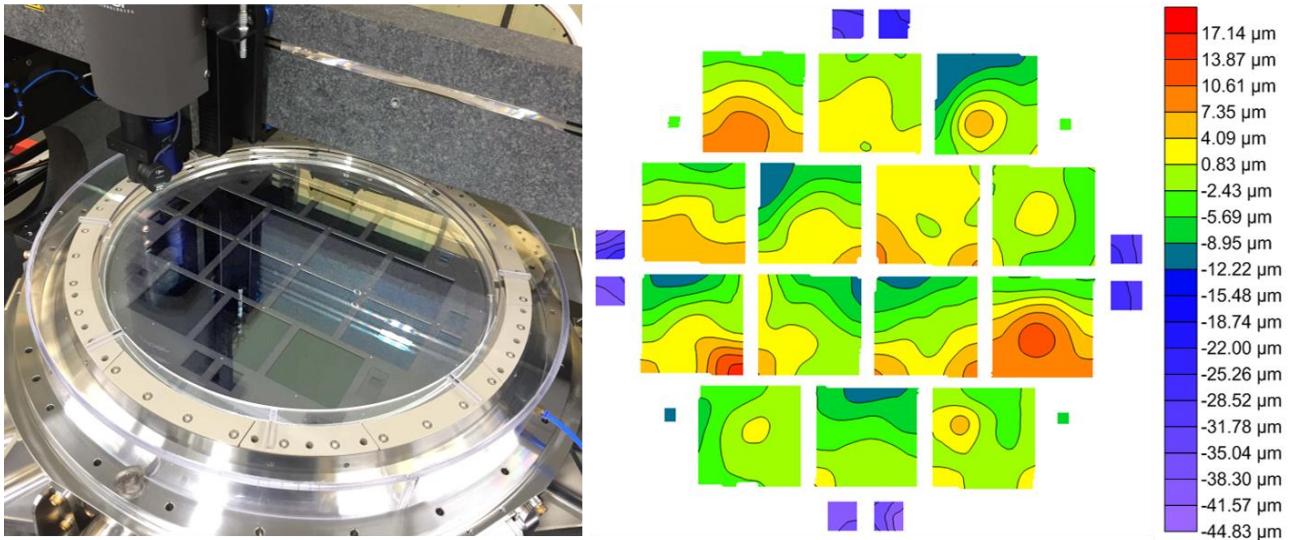


Figure 4 The focal plane inside the cryostat and flatness measurements made at -110 °C showing the fourteen science devices, eight wavefront and four autoguide CCDs.

4. THE INSTRUMENT CONTROL AND SUPPORT SUBSYSTEM

4.1 Instrument Control and Support Subsystem Description

A pair of liquid nitrogen Dewars, together with associated valves etc., is mounted on the telescope fork. The temperature control and other control functions are implemented through a Programmable-Logic-Controller (PLC) system. Cold plate temperature control is achieved by controlling the rate of flow of gaseous nitrogen emerging from the cryostat. No electrical heaters are included on the cold plate assembly. PT1000 temperature sensors are distributed around the cold plate. The temperature used for control (the control temperature) is calculated by taking the median of the mean of the central sensors and the mean of the outer sensors. PID control is employed but, as this is a slowly responding system, only the proportional and integral terms are used. Initial values were set using the Ziegler–Nichols method and based on the step response to the flow rate. The time constant of the cold plate response (~3.5 hours) is consistent with dynamic modelling results.

4.2 Thermal Performance

Thermal trials have been undertaken on an engineering model system with representative heat loads controlled by applying heat to the window assembly using resistive heaters. The plate temperature (the control temperature) during a week of operation is shown in Figure 5. During this time the radiative heat load was varied between 55 and 100 Watts at a maximum rate of change of 4.5 Watts/hour. The required temperature stability is +/- 1 °C over a period of one week. The largest plate temperature deviations occur during Dewar fill. Even including the Dewar fill, it has been demonstrated that these requirements have been met. Excluding the two hours following Dewar fill the plate temperature stability is better than +/- 0.5 °C over the expected range of operating conditions. The time taken to achieve a stable cold plate temperature of -110 °C from room temperature under controlled cooldown conditions is less than 12 hours. Warm-up to ambient takes in the order of 24 hours.

The uniformity of the temperature across the cold plate is also important in this application. At a set temperature of -110 °C the temperature deviation across the cold plate is better than 2.5 °C, significantly within the requirement of 10 °C.

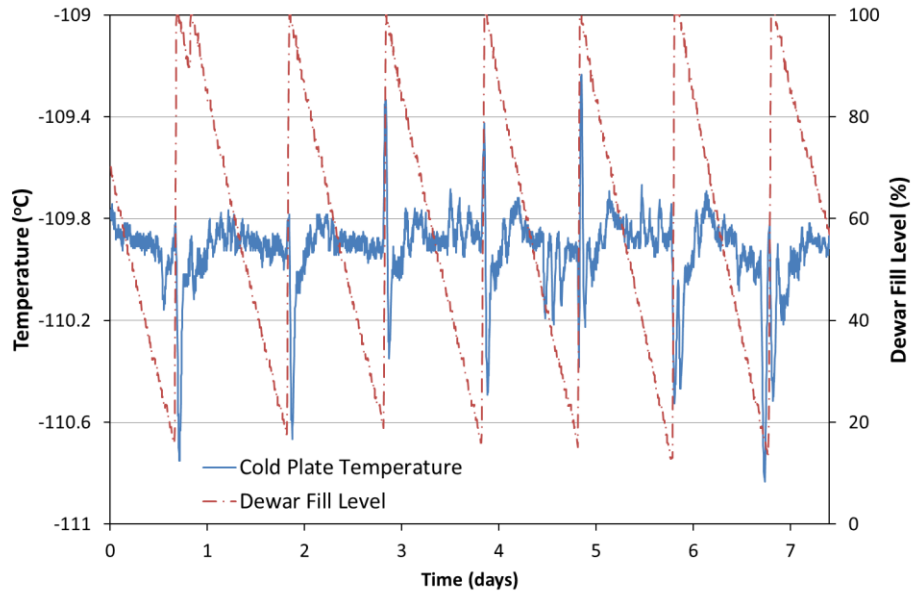


Figure 5 The control temperature and the Dewar fill level

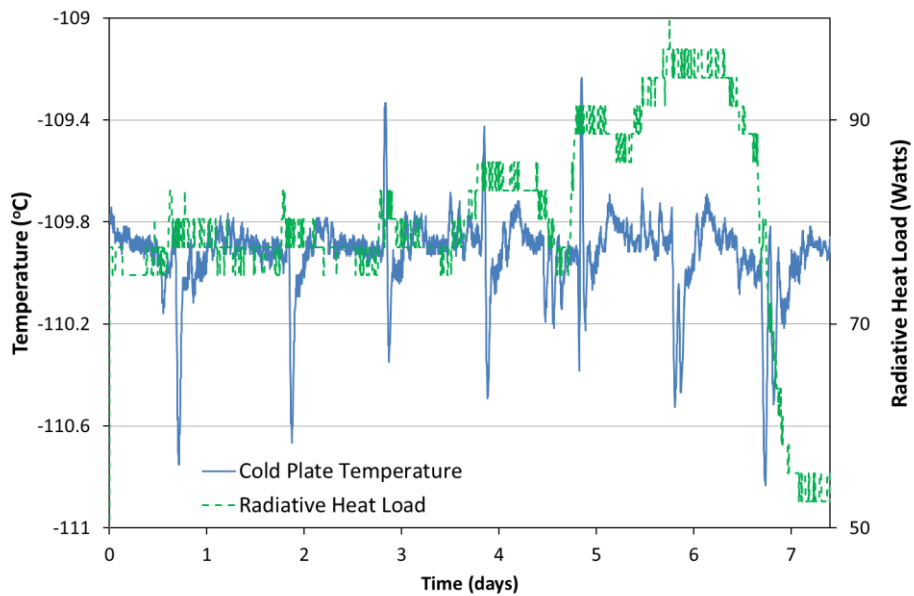


Figure 6 The control temperature and the radiative heat load on the cold plate

4.3 Vacuum Performance

One of the key requirements of the Cryocam system is to provide high system availability so that the time to complete the total survey by the end user is as short as possible. Therefore, as well as designing the system for high reliability, the impact of regenerating the sorption pump material must be minimised. Careful attention has been paid to the design of the cryostat to ensure suitable vacuum performance can be achieved, for example by the choice of materials and

processes used, and the elimination of virtual leak sites where possible. From a vacuum perspective some non-optimal choices have had to be made for practical reasons, for example the use of Viton seals. Any epoxys used, such as those for die attach, have been chosen for their excellent outgassing characteristics.

Only the bake-out of the Viton seals and the sorption pump material was undertaken prior to the testing activity at e2v. No full system bake-out was undertaken. The entire system will be thoroughly conditioned just before it leaves the factory and once again on site. Figure 7 shows the vacuum performance without the full bake out. The cold plate was cooled to -110°C and sorption pump material to -186°C . Once the cold plate had reached the required temperature (-110°C) and stabilised the turbo-pump was turned off and the vacuum pressure observed whilst the system was running on sorption pump only. The variation in vacuum pressure tracks the cryostat body temperature which was varying due a changing ambient temperature. This implies that there is a gas load coming from the outgassing of the cryostat walls etc. which will be greatly reduced by full cryostat conditioning. In its present state the gas load is dominated by water vapour, confirmed by the use of a mass spectrometer for residual gas analysis of the system. The vacuum pressure required to maintain the thermal performance of the cryostat is only around 10^{-3} mbar. However, we aim to keep the pressure below $\sim 10^{-5}$ mbar to ensure the water vapour does not condense on the focal plane at a cold plate temperature of -110°C .

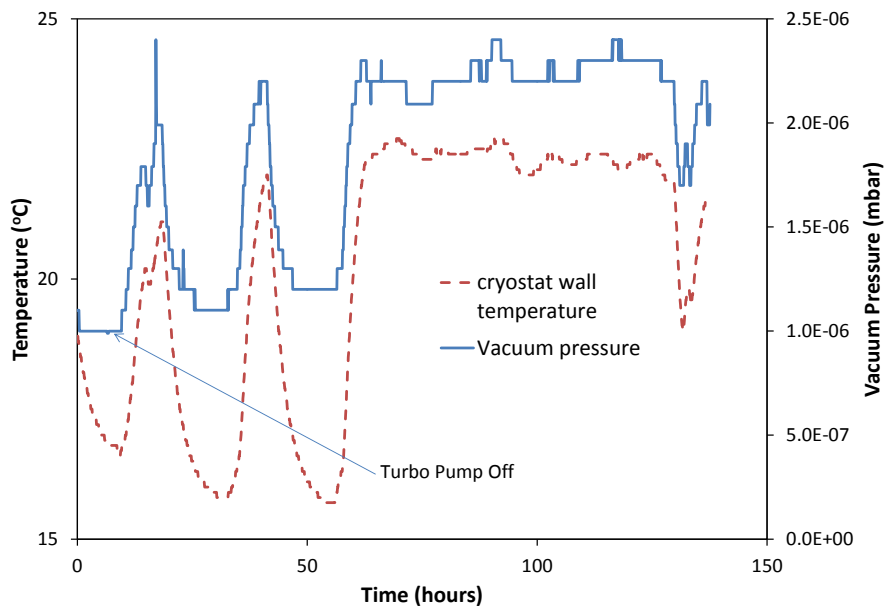


Figure 7 The vacuum pressure whilst running on sorption pump only. The dashed line is the temperature of the cryostat wall which is following the ambient temperature.

To reactivate the sorption pump, material once the vacuum performance can be no longer maintained, requires it to be heated to around room temperature, whilst the system is being pumped with a turbo pump. The warm up and cool down process can be undertaken within 15 hours with only a 1.5°C deviation in plate temperature.

5. DETECTOR CONTROL SUBSYSTEM

5.1 Electronics overview

The JPAS drive and data acquisition sub system comprises 22 local drive modules providing optimised drive circuitry, front end electronics for low noise performance, and a local frame store. Data is combined within an interface module which receives control commands, and delivers the image data to the user via a fibre optic link. There are 94 programmable devices within the subsystem comprising 70 FPGAs and 24 CPLDs, containing 13 different designs. A schematic of the detector control subsystem is presented in Figure 8.

All CCDs are connected to its drive module via short flexi connections through a feedthrough arrangement at the base of the cryostat. The drive modules digitise the CCD signals and each one is coupled to the interface module. Digital correlated double sampling is employed to optimise the noise performance. Because this large mosaic has 224 channels

of science data to digitise, in close proximity to the auxiliary sensors, a differential CCD output is used for readout of the science devices. A detailed discussion on the use and performance of digital CDS is given in [3].

Four fibre-optic cables link the CCD electronics to the host computers.

Four modes of full frame operation of the science devices are available to the end user, un-binned and binned at pixel rates of 400 and 633 pixels per second per output.

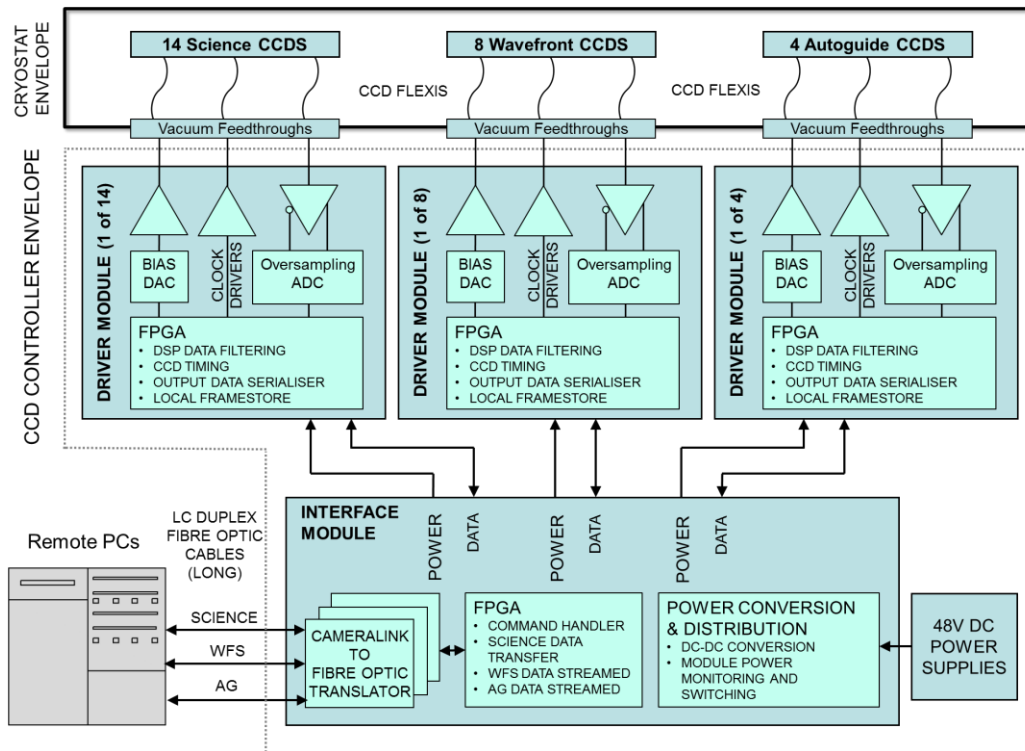


Figure 8 A schematic of the detector control sub system

5.2 Electrical Performance

Electrical/electro-optical performance has been assessed at the device level, module level and system level to ensure that the customer requirements can be met. The following sections summarise these key verification activities.

5.2.1 CCD level performance

An example of an e2v CCD290-99 science device [4], together with its schematic layout, is shown in Figure 9. All the CCDs used are rigorously tested individually and are supplied into the system as high grade devices. Device testing was undertaken on e2v standard production test systems. Each output of the science devices was operated at a pixel rate of 500 kpixels/s/output. The device temperature was -100°C , around the expected operating temperature. A conventional analogue CDS video chain was employed giving a mean noise performance over all outputs and devices of 3.4 electrons. This is a single ended result. Operating using differential CCD output increases the noise figure by $\sqrt{2}$, giving a figure of 4.8 electrons.

The small signal Charge transfer efficiency (CTE) was measured using Fe55 x-rays. The Serial CTE was better than 0.999994, with a parallel CTE better than 0.999999. The CCD290-99 devices use deep depletion silicon, back-thinned with a multilayer AR coating for maximum sensitivity and optimised over the desired 360 to 885 nm range. A summary of the production measurement of the quantum efficiency from all the science devices is presented in Figure 10.

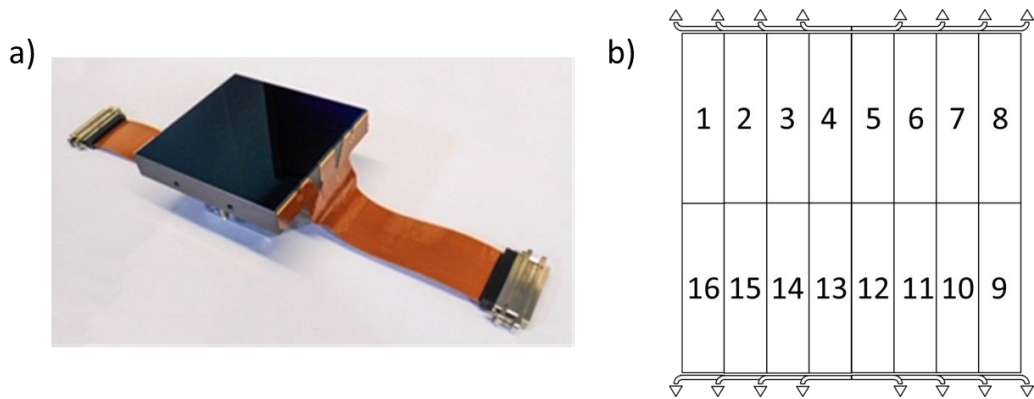


Figure 9 (a) A CCD290-99 science device showing the flexi connections and (b) the device layout.

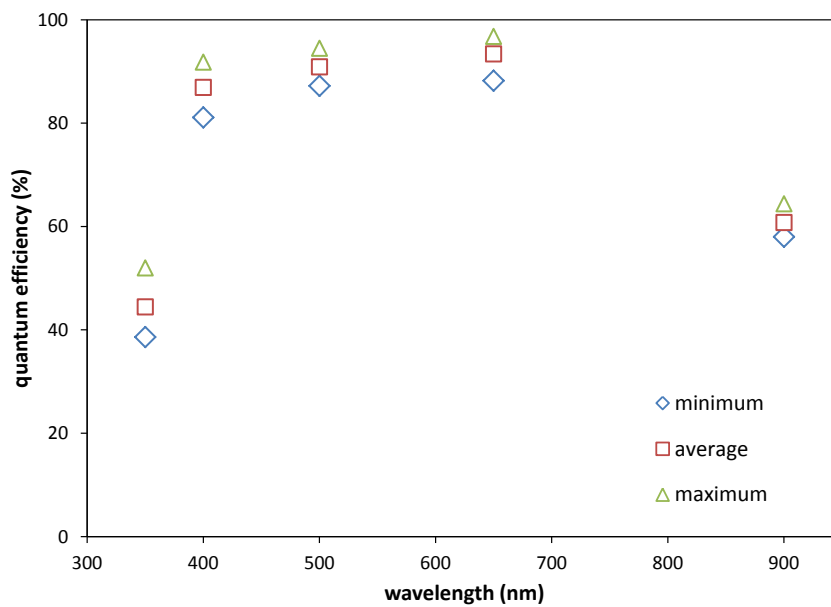


Figure 10 A summary of the measured quantum efficiency over all of the science devices.

5.2.2 Module level performance

The electronics modules were bench tested using test devices (science, wavefront or autoguide) mounted in a purpose built cryostat and cooled using liquid nitrogen. This enabled detailed characterisation and the production testing of every module. Photon transfer curves were obtained to test the gain from every output and the charge transfer efficiency was measured using the EPER technique to check for any clocking issues.

An example of the noise performance of all 16 outputs of a science module transferring in parallel is given in Figure 11. One ADU corresponds to 2.2 ± 0.1 electrons and the mean measured noise from this particular module is 4.3 electrons.

As part of the science module characterisation exercise the electrical cross talk between the outputs was assessed by illuminating a section of the test device with a well-defined spot pattern and observing any occurrence of signal from the other outputs. No cross talk was observed above the noise of the measurement technique, giving a minimum cross talk rejection ratio better than $\sim 100\text{dB}$.

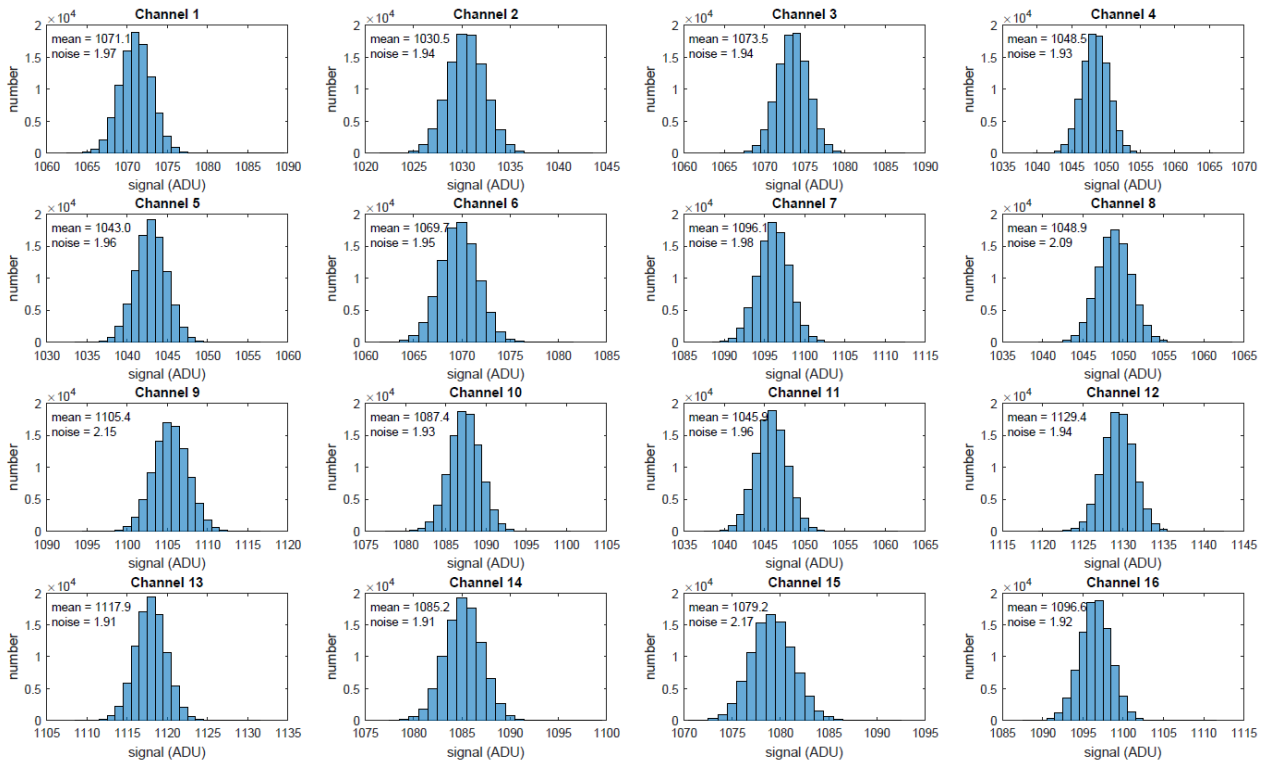


Figure 11 The measured noise performance of a science module operating at a pixel rate of 400 kpixels/s per output

5.2.3 System level performance

The individual electronics modules are all mounted at the rear of the cryostat and each directly plugged into a vacuum feedthrough to make connection with its associated CCD inside the vacuum envelope. Around 1.4 kW is dissipated by the electronics and the heat is extracted from each module through a heat pipe arrangement, thermally connected to a common water/glycol cooled cold plate. Special consideration has been made to the mechanical design to ensure ease of build and replacement of modules if necessary. The rear view of the cryostat showing the installed modules and the interface module is presented in Figure 12.

System level electrical performance testing has been undertaken to ensure compliance with requirements. This includes detailed noise and cross talk assessment and functional assessment. Two methods were employed to provide optical stimulation of the CCDs. Firstly, an array of LEDs was mounted outside the cryostat in the implosion shield protecting the optical window. An LED was located directly above the centre of each CCD. Powering each LED in turn enabled confirmation of the CCD position and basic functionality. The second method utilised a pinhole camera arrangement of Figure 13 a). This used a 0.5 mm pinhole which gave a resolution on the focal plane significantly better than 2 mm. The first image obtained from Cryocam, with all the science devices reading out in parallel is shown in Figure 13b).

Low system noise is a very important requirement for this application. Quantitative assessment of the noise was undertaken in the dark under various modes of operation. The noise performance from the science devices, all reading out in parallel and with the auxiliary devices running (i.e. under worst case conditions) is shown in Figure 14. Here, for every science device, the noise from each of the 16 outputs is plotted against output number. The measurements are consistent with the measurements from individual modules made on the bench as part of the production tests. The performance is significantly better than the customer requirements, enabling improved science to be performed by the end user.

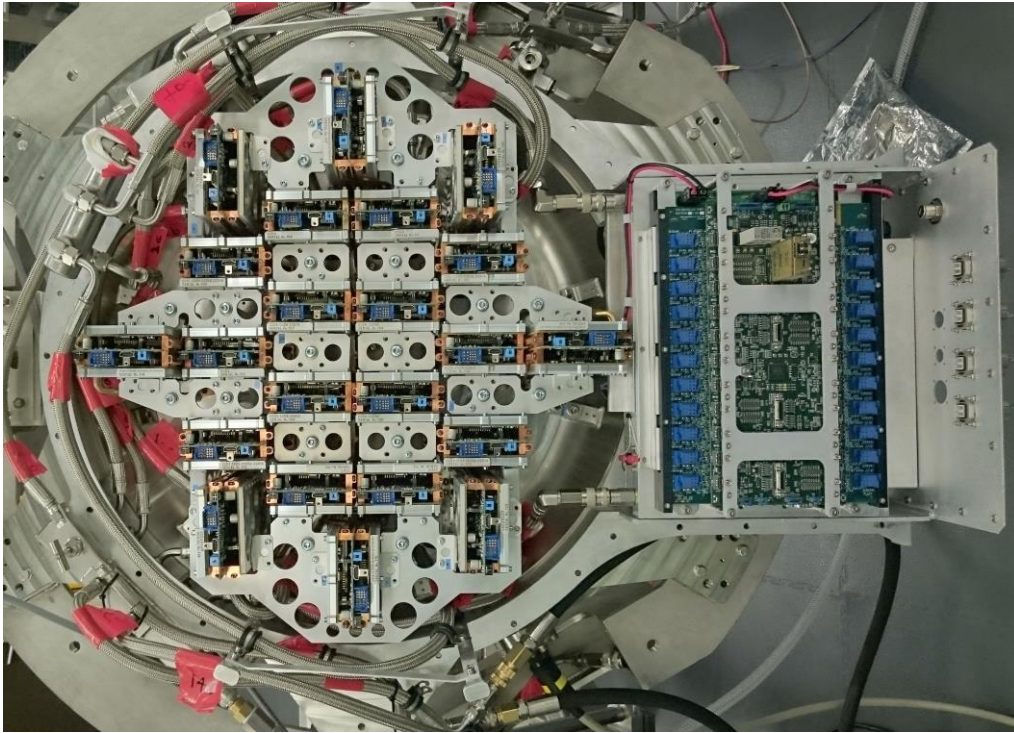


Figure 12 All the science, wavefront and autoguide modules, together with the interface module mounted on the rear of the cryostat prior to cable attachment and cover mounting.

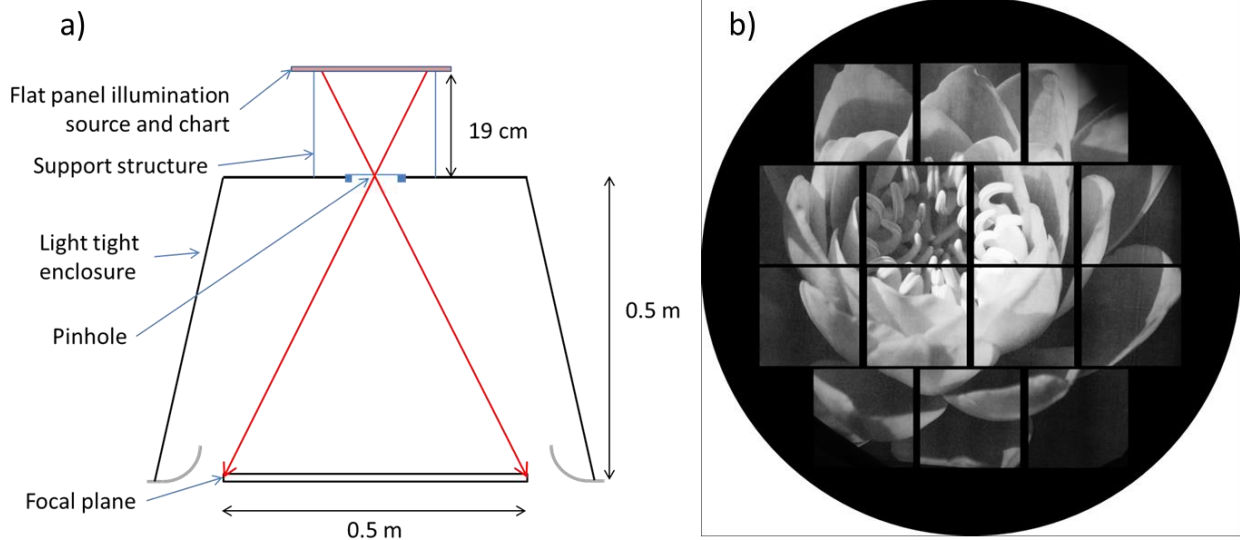


Figure 13 a) The pinhole camera projection arrangement for qualitative imaging assessment, b) The first test image taken with the deliverable Cryocam: 60s integration time and all devices readout in parallel.

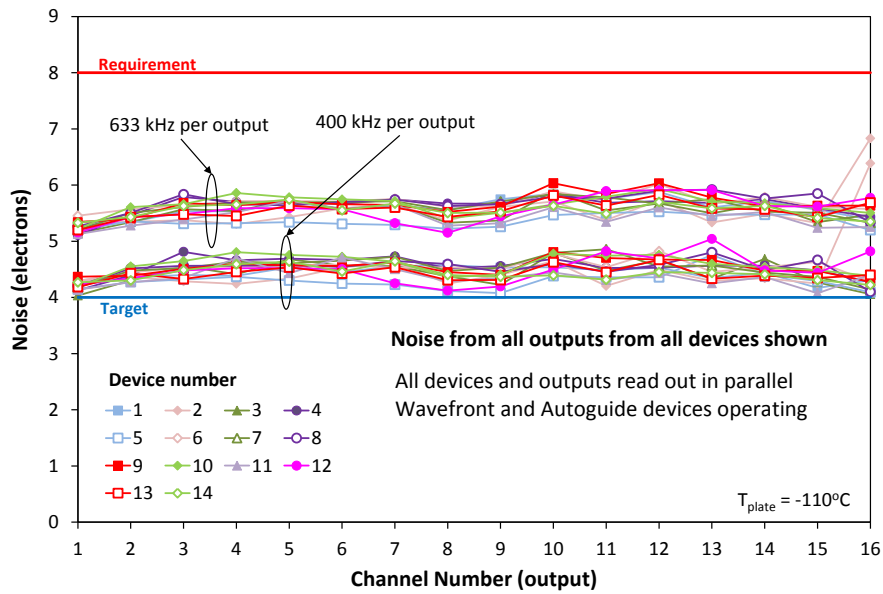


Figure 14 The measured system level noise for all science devices operating in parallel at a pixel rate of 400 and 633 kpix/output/second. All wavefront and autoguide devices are also operational. The elevated noise measured from output 16 of device 2 was seen during device testing

Reliability and stability of operation is also critical to ensure efficient data acquisition and to minimise the total survey time. The stability is demonstrated by the noise measurements made over an extended period of time, the data being taken during EMC testing of the system. The noise measured from the science devices over a 6-day period is shown in Figure 15.

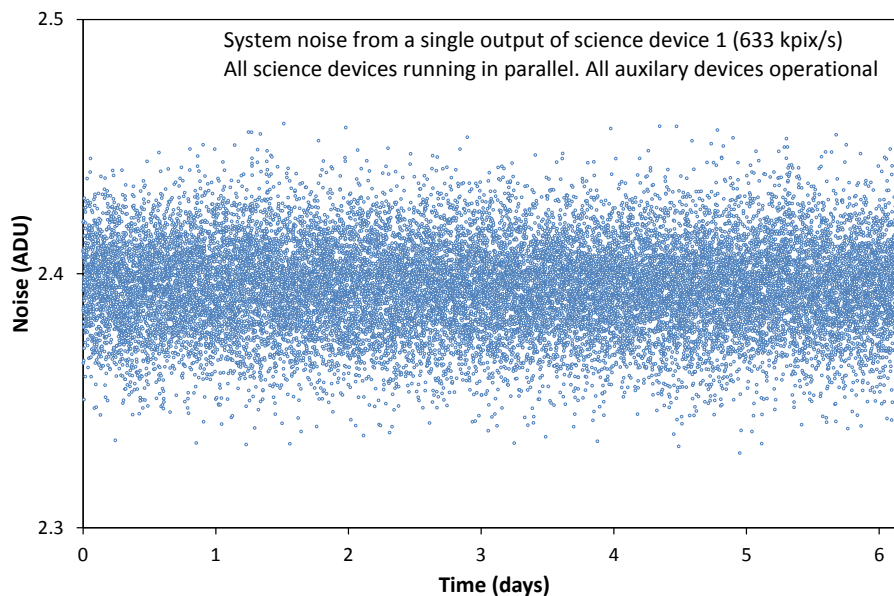


Figure 15 The system noise from a single science output measured over a 6-day period showing the excellent stability achieved. All devices are operating and image capture and noise measurement is made every 25 seconds.

As many devices are operating with multiple outputs at high speed there is a risk of significant cross talk between outputs and devices unless carefully considered during the design. For example, cross talk has been eliminated by using

synchronous clocking of all science devices and making use of the differential outputs. At the module level, cross talk between outputs was assessed optically, as described in the previous section. At the system level this was not possible as significant background signal was generated through reflection from the engineering window, which was not AR coated. As an alternative, the cross talk signal generated from a bright defective column in one of the science devices was investigated. The signal was averaged across all rows of a device for all science devices at the same column location as the column defect. No cross talk could be seen within the noise, giving a minimum cross talk rejection of 106dB. A similar level of rejection was seen between outputs of the same device, confirming the measurements made at the module level.

6. LESSONS LEARNED

In addition to the number of advanced technical developments to be undertaken it is clear that the successful delivery of a programme such as this is also dependent on a rigorous system engineering approach and the adherence to a robust quality process. For example, working with the customer to generate a detailed set of system requirements has proved to be crucial, as has the implementation of a controlled process to accommodate request for change in the requirements. Clearly defined review points have proven to be very useful to ensure the program remains on track technically and to schedule, such as the major customer reviews (PDR, CDR etc.) and internal reviews for each part of the build (manufacturing readiness reviews, test readiness reviews etc.). A process of progressive verification has enabled requirements to be sold off throughout the programme, addressing risk items as soon as possible and eliminating the need for a lengthy factory acceptance review.

7. CONCLUSIONS

The e2v Cryocam programme is currently in its final verification phase with factory acceptance planned for June 2016. From the final critical design review it has taken 15 months to complete the complex AIVT phases of the programme. System level tests have verified performance against all key aspects of the customer requirements, including the cooling performance, geometric requirements, including the flatness of the focal plane, and the noise and cross talk performance of the electronics. Key features include

- Exceeding the focal plane flatness specification to achieve 27 μm peak to valley flatness, operating cold.
- Precision construction and metrology of the instrument to meet geometrical/mechanical specifications.
- Validating the differential digital correlated sampling signal chain to provided guaranteed read-noise that exceeded specifications.
- Custom liquid nitrogen cryogenic/vacuum system for reliable and low maintenance operation.

We have demonstrated that the supply of a complex, high performance camera system can be undertaken by a commercial organisation. This includes the use of rigorous quality systems, delivering guaranteed performance levels, as well as to an agreed price and schedule.

8. ACKNOWLEDGEMENTS

In addition to the dedicated core team at e2v many other colleagues have contributed material and expertise to this work. The J-PAS collaboration is extensive and thanks go to all who have continued valuable discussions as this project progresses. CEFCA plays an important role as host of the telescope.

REFERENCES

- [1] K. Taylor et al., "JPCAM: A 1.2 GPixel Camera for the J-PAS Survey" JAI, vol 3, No 1 (2014) 1350010
- [2] P. R. Jordan, et al., "A gigapixel commercially manufactured cryogenic camera for the J-PAS 2.5m survey telescope", Proceedings of SPIE Vol. 8453, 84530J (2012)
- [3] M. J. Clapp, "Development of a test system for the characterisation of DCDS CCD readout techniques", Proceedings of SPIE Vol. 8453, 84531D. (2012)
- [4] <http://www.e2v.com/products/imaging/>